Comparative Biochemistry and Physiology, Part A 188 (2015) 120–126

Contents lists available at ScienceDirect

Comparative Biochemistry and Physiology, Part A

journal homepage: www.elsevier.com/locate/cbpa

Renal plasticity in response to feeding in the Burmese python, *Python molurus bivittatus*

A.J. Esbaugh [a,*], S.M. Secor [b], M. Grosell [c]

[a] Department of Marine Science, University of Texas at Austin, Marine Science Institute, 750 Channel View Drive, Port Aransas, TX 78418, USA
[b] Department of Biological Sciences, University of Alabama, Tuscaloosa, AL 35405, USA
[c] Division of Marine Biology and Fisheries, University of Miami, Rosenstiel School of Marine and Atmospheric Science, 4600 Rickenbacker Causeway, Miami, FL 33149, USA

ARTICLE INFO

Article history:
Received 13 April 2015
Received in revised form 13 April 2015
Accepted 23 June 2015
Available online 27 June 2015

Keywords:
Alkaline tide
Specific dynamic action
V-type ATPase
Carbonic anhydrase
CA IV
Kidney
Acid–base balance

ABSTRACT

Burmese pythons are sit-and-wait predators that are well adapted to go long periods without food, yet subsequently consume and digest single meals that can exceed their body weight. These large feeding events result in a dramatic alkaline tide that is compensated by a hypoventilatory response that normalizes plasma pH; however, little is known regarding how plasma HCO_3^- is lowered in the days post-feeding. The current study demonstrated that Burmese pythons contain the cellular machinery for renal acid–base compensation and actively remodel the kidney to limit HCO_3^- reabsorption in the post-feeding period. After being fed a 25% body weight meal plasma total CO_2 was elevated by 1.5-fold after 1 day, but returned to control concentrations by 4 days post-feeding (dpf). Gene expression analysis was used to verify the presence of carbonic anhydrase (CA) II, IV and XIII, Na^+ H^+ exchanger 3 (NHE3), the Na^+ HCO_3^- co-transporter (NBC) and V-type ATPase. CA IV expression was significantly down-regulated at 3 dpf versus fasted controls. This was supported by activity analysis that showed a significant decrease in the amount of GPI-linked CA activity in isolated kidney membranes at 3 dpf versus fasted controls. In addition, V-type ATPase activity was significantly up-regulated at 3 dpf; no change in gene expression was observed. Both CA II and NHE3 expression was up-regulated at 3 dpf, which may be related to post-prandial ion balance. These results suggest that Burmese pythons actively remodel their kidney after feeding, which would in part benefit renal HCO_3^- clearance.

1. Introduction

Many animals feed intermittently and therefore experience extended episodes of fasting between potentially large meals. Extreme examples of this are the sit-and-wait foraging snakes (e.g., pythonids, boids, and viperids) whose meals range from 25–160% of their body weight, and occur at average intervals of approximately 1–3 months (Pope, 1961; Slip and Shine, 1988; Secor and Nagy, 1994; Greene, 1997). This feeding pattern has led to a number of unique adaptations involving the capacity to regulate digestive performance and nutrient uptake. One hallmark of the digestive physiology of these snakes is an impressive specific dynamic action – the extra energy expended on meal digestion and assimilation – owing to the exceptional effort to breakdown and assimilate their large intact prey (Secor and Diamond, 1997a, 2000; Toledo et al., 2003; Secor, 2009). After these snakes complete digestion their stomachs shut down acid production, intestinal hydrolases and transporters are down-regulated, and the small intestine atrophies (Secor and Diamond, 2000; Secor, 2003; Ott and Secor, 2007; Cox and Secor, 2008).

Another phenomenon found in sit-and-wait predators is the presence of a pronounced post-prandial alkaline tide, which is an increase in plasma pH and/or HCO_3^- that occurs in parallel with digestion. This results from the equimolar transport of H^+ and HCO_3^- from the oxyntopeptic cells into the stomach and plasma, respectively (reviewed by Wang et al., 2001). Despite the post-prandial increase in plasma HCO_3^-, pythons are able to successfully defend plasma pH via a relative hypoventilatory mechanism (Overgaard et al., 1999; Hicks et al., 2000; Secor et al., 2000; Wang et al., 2001; Andrade et al., 2004; Arvedsen et al., 2005) whereby the relative amount of exhaled CO_2 is lower than would be expected based on the increased metabolic rate. This compensatory respiratory acidosis stabilizes plasma pH at normal levels. Respiratory compensation is regarded as the primary mechanism that air-breathing vertebrates use to correct plasma acid–base disturbances, largely owing to CO_2 based ventilatory drives and high blood CO_2 capacitance.

While respiratory compensation effectively corrects plasma pH, it does not act to reduce the elevated plasma HCO_3^-. In many vertebrates this function is performed by kidneys through renal acid–base transport pathways. Typically, plasma HCO_3^- is filtered by the glomerulus and the majority is subsequently reabsorbed in the proximal tubule. Reabsorption involves transport of protons into the proximal tubule lumen by sodium hydrogen exchanger 3 (NHE3). In the proximal tubule luminal, carbonic anhydrase IV (CA IV) quickly catalyzes the dehydration of HCO_3^- to CO_2, which diffuses back into the epithelial cells. Cytoplasmic

* Corresponding author. Tel.: +1 361 749 6835; fax: +1 361 749 6749.
E-mail address: a.esbaugh@austin.utexas.edu (A.J. Esbaugh).

http://dx.doi.org/10.1016/j.cbpa.2015.06.029
1095-6433/

CA hydrates CO_2 back into HCO_3^-, which is transported through the basolateral Na^+, HCO_3^- co-transporter (NBC) into the blood while the resulting proton is recycled back into the lumen. During periods of metabolic alkalosis this system can act to limit HCO_3^- reabsorption and thereby lower plasma HCO_3^-. Additionally, renal compensation can also occur via HCO_3^- secretion in the collecting duct system. In this instance intracellular CA hydrates CO_2 to form HCO_3^-, which is transported into the lumen of the collecting duct through an apical anion exchange protein. The resulting proton is transported through basolateral V-type H^+ ATPase. Interestingly, the renal involvement with regard to post-prandial acid–base compensation in snakes has yet to be investigated. The available information regarding the role of renal compensation in reptiles is mixed. Alligators are completely void of the required cellular machinery for acid–base compensation – most notably CA and NHE activity (Ventura et al., 1989) – and both turtles and water snakes do not respond to a systemic acidosis (Dantzler, 1968; Silver and Jackson, 1986) with renal adjustments. Conversely, water snakes do appear to contain renal CA activity, respond to an alkalosis and have the capacity for basolateral pH_i regulation in the proximal tubules (Dantzler, 1968; Kim and Dantzler, 1995a,1995b; Dantzler et al., 1999).

On this background, the current study investigated the potential role and re-modeling of the Burmese python kidney in response to the dramatic alkaline tide that occurs post-feeding. In particular, we used gene expression to ascertain the presence and transcriptional regulation of six genes relevant for renal HCO_3^- transport — CA II, CA IV, CA XIII, NHE3, NBC and the V-type ATPase β subunit. Further enzymatic characterization of CA and V-type ATPase activity were used as phenotypic anchors for gene expression results. We hypothesized that not only would Burmese pythons have the cellular machinery for renal HCO_3^- regulation, but also that the post-prandial pythons would down-regulate the components required for HCO_3^- reabsorption, most notably luminal CA IV activity to aid clearing of accumulated HCO_3^- during the alkaline tide.

2. Materials and methods

2.1. Experimental animals and sampling

Care of, and experimentation on snakes was approved by the Institutional Animal Care and Use Committees of both the University of Alabama and the University of Miami. Captive-born hatchling pythons were purchased commercially and housed individually in 20-liter plastic containers at 27 °C under a 14 h:10 h light:dark cycle. Snakes (both male and female) were fed laboratory rats every 2 weeks and had continuous access to water. Prior to the study 18 pythons (mean ± S.E.M = 501 ± 10 g) were fasted for approximately 30 days to insure they were post-absorptive (Secor and Diamond, 1995). Six snakes remained fasted for the study and 12 pythons were fed a single prekilled rat weighing approximately 25% of the snake's body mass. Snakes were euthanized fasted or at 1, 2, 3, 4 days postfeeding (dpf) by severing their spinal cord immediately posterior to the head. From a mid-ventral incision blood was sampled directly from the severed left systemic artery and kidney tissues were excised. Blood samples were immediately centrifuged and the plasma frozen in liquid nitrogen. Note that this method is not suitable for plasma pH and P_{CO2} measurement, so samples were only used to measure total CO_2 as a proxy for retained HCO_3^-. Tissue samples were likewise frozen with liquid nitrogen and all samples were subsequently stored at −80 °C.

2.2. Molecular methods

Total RNA was extracted from python kidneys using RNA Stat-60 reagent (Tel-test Inc, TX, USA.) according to manufacturer guidelines. Tissue was first powdered on liquid nitrogen using a mortar and pestle, followed by motor driven homogenization. Total RNA was quantified using an ND-1000 (Thermo Fisher Scientific, DE, USA.) spectrophotometer at a wavelength of 260 nm. Prior to cDNA synthesis, a subsample of RNA was DNase-treated with amplification grade DNase I (Invitrogen, CA, USA; manufacturer specifications) to remove potential DNA contamination. cDNA synthesis was performed using RevertAid MULV reverse transcriptase (Fermentas, MD, USA.), according to manufacturer specifications. Degenerate primers were designed for cytoplasmic CA IV, NBC and the V-type H^+ ATPase by aligning available sequences from a diverse array of vertebrates and identifying conserved nucleotide regions (Table 1). PCR reactions were performed according to standard protocols using commercial Taq DNA polymerase and buffer (Qiagen, CA, USA.). PCR products were subsequently gel extracted using the Qiaquick kit (Qiagen, CA, USA.), cloned (TOPO TA cloning kit; Invitrogen, CA. USA.) and sequenced. Primers for rapid amplification of cDNA ends (RACE) and real-time PCR were designed using the fastpcr freeware program (Table 1). RACE libraries were generated using the SmartRace cDNA synthesis kit (Clontech, CA, USA). Real-time PCR was performed on an Mx3000P real-time PCR system (Stratagene, CA, USA.) using the Brilliant SYBR green master mix kit (Stratagene, CA, USA.; 12.5 μl reactions). Both the thermocycler set-up and reaction composition were performed according to manufacturer guidelines, and a disassociation curve was used to assess the primer specificity of each reaction. The PCR efficiency of each primer pair was calculated using a cDNA standard curve. PCR efficiencies ranged from 96–114% with an $R^2 \geq 0.98$. Relative mRNA expression was calculated using the delta-delta ct method using elongation factor 1α (ef1α) as an internal control and the fasted treatment as the relative control (Pfaffl, 2001). Successful DNase treatment was verified using a no reverse transcriptase control for each tissue set.

2.3. Biochemical methods

CA activity was measured using the electrometric delta pH method (Henry, 1991). Briefly, the reaction medium consisted of 2.5 ml of buffer (225 mM mannitol, 75 mM sucrose, 10 mM Tris base; Sigma, MO, USA.) kept at 4 °C. Biochemical assessments of python and bovine red blood cell CA were performed using 2 ml of buffer. The reaction was started by adding 100 μl of CO_2 saturated Milli-Q water using a gas tight Hamilton syringe. The reaction rate was measured over a pH change of 0.15 units (+10 mV). To calculate the true catalyzed reaction rate, the uncatalyzed reaction rate was subtracted, and the buffer capacity was used to convert the rate from mV into mol H^+ per unit time. The

Table 1
List of primers used for real-time and degenerate PCR. All sequences are 5′ to 3′ and reverse primers are reverse compliments of the genetic sequence.

Application	Gene		Sequence
Degenerate	CA IV	F	CCA TGG AGN TGC AYA TMG T
		R	GGT GTK GTN AGN GAG CC
	ATPase	F	CNG CAN TGG GNG TNA ACA TGG
		R	GNG GRT ARA TCT GTC KGT TRT G
	NBC	F	TGG AAG GAG CAN GCN AGG TGG
		R	CTC TCC AAC ACR CCC TGC ATG
Real-time	CA II	F	ATG TCC TGG GGC TAC AGC AA
		R	GTG CAG GAT CGA ACT TGG CA
	CA IV	F	GCG ATC AAA GGA AAA GGC GTA GCA G
		R	GAT CCC AGG GCC AAA GCT GG
	CA IV-like	F	CAT TGT GGT CCT AAA ACA TGG AT
		R	GCT GTT CTC ATA ACC AAC CAG AG
	CA XIII	F	GTT GAA GCT GCT CGG CAA TCT G
		R	GGG ACT GTG AGA GAC CCA AGG
	ATPase	F	GGT GAT CTT GAC CGA CAT GAG C
		R	GCG TGA TGG AGC CAT TCC TG
	NBC	F	CCT ACC ACTG AAA TTG GAC GAG CCA
		R	CAG GAT CCC ATT CCC CAG GAG
	Ef1α	F	TCT CGA TTC TGT GGG TGG T
		R	CTC AAT CTC GTG TGG CTG A

pH was measured using a PHC4000 combined pH electrode (Radiometer Analytical, Lyon, France) attached to a PHM220 lab pH meter (Radiometer Analytical, Lyon, France).

Kidney samples were cut into small pieces using a razor blade after which they were homogenized in 10–20 volumes of CA assay buffer using a motor driven Teflon glass homogenizer. The crude homogenate was then differentially centrifuged as described by Henry et al. (1993), which involved an initial spin of 7500 g for 20 min to remove intact cells, nuclei, mitochondria and large cell fragments. The resulting supernatant was then centrifuged at 100,000 *g* for 90 min to separate membrane (pellet) and cytoplasmic (supernatant) fractions. Cytoplasmic fractions were assayed for CA activity, while membrane fractions were washed to remove potential contaminating cytoplasmic CA activity. The washing protocol consisted of re-suspended the membrane pellet in approximately 35 ml of CA assay buffer, sonicating the solution (3 × 5 sec pulses) and re-centrifuging the sample (Esbaugh and Tufts, 2004; Esbaugh et al., 2009a). Final washed pellets were re-suspended in assay buffer at a ratio of 100 mg:1.5 ml and assayed for CA activity. Membrane fractions were tested for the presence of a GPI-linked CA using the specific cleaving enzyme phosphotidyl inositol phospholipase C (PI-PLC; Sigma, MO, USA.). Exposure of membranes containing GPI-linked CA to PI-PLC should cause the release of CA from the membranes, and thus activity would be found in the supernatant after membrane re-isolation. For PI-PLC experiments, each sample was separated into two 1.5 ml aliquots and either 1 unit of PI-PLC or vehicle (CA assay buffer) was added to each sub-sample. The reactions were left at room temperature (23 °C) for 60 min, after which the membranes were re-isolated by centrifugation and the resulting supernatant was examined for released CA activity.

V-type H^+ ATPase activity was measured in kidney samples using a coupled enzyme ATPase protocol (McCormick, 1993), as modified for V-type H^+ ATPase (Lin and Randall, 1993; Kultz and Somero, 1995). Tissue samples were homogenized on ice in SEID buffer (150 mM sucrose, 10 mM Na_2EDTA, 50 mM imidazole, 0.1% sodium deoxycholic acid; Sigma, MO, USA.) using a motor driven homogenizer. Samples were then briefly centrifuged at 5000 *g* for 1 min to pellet larger material. The final assay concentration of *N*-ethymaleimide (Sigma, MO, USA.) was 1 mM, and 10 μl of sample was used for activity determination. The consumption of NADH was measured using a plate spectrophotometer (Molecular Devices, CA, USA.) at a wavelength of 340 nm over the 15 minute interval immediately after the addition of sample and assay reagent.

All enzyme assay results were normalized to total protein content, which was detected using a commercially available Bradford assay reagent (Sigma, MO, USA.). Total CO_2 of plasma samples was measured using a Corning 965 total CO_2 analyzer.

2.4. Phylogenetic analysis

A total of 45 membrane-associated CA sequences were mined from Genbank, which included isoforms from all five vertebrate classes. Phylogenetic analyses were performed using MEGA version 6.06 and amino acid sequences were aligned using the MEGA Clustal alignment tool. Three analyses were performed: 1) neighbor joining (NJ), 2) maximum parsimony (MP) and 3) maximum likelihood (ML). Gaps were treated as complete deletion for parsimony and likelihood methods and pairwise deletion for neighbor joining methods. MP was performed using the subtree-pruning-regrafting (SPR) method, while ML was performed using a Jones–Taylor–Thornton (JTT) substitution model. Both methods used the MEGA default tree inference options. NJ was performed using the Poisson substitution model. Support for nodes in all analytical procedures was performed via bootstrap analysis with 1000 replications. For all resulting trees, the *Drosophila melanogaster* CA sequences was used to root the analysis. No partial sequences were included in the analysis.

2.5. Statistics

All comparisons of gene expression and enzyme activity between fasted and 3 dpf pythons were performed using an unpaired Student's *t*-test. In cases where normality was not met, a non-parametric Mann–Whitney rank sum test was performed. A paired *t*-test was used to assess the effectiveness of PI-PLC at cleaving CA from membranes as compared to no enzyme control. A one way analysis of variance (ANOVA) with a Dunnett's post-hoc test was used to compare plasma total CO_2 levels of fed versus fasted animals. An analysis of covariance (ANCOVA) was used to assess kidney wet weight relative to body weight in fed and fasted animals. A fiducial level of significance of 0.05 was used for all statistical analyses.

3. Results

3.1. Effects of feeding

As expected, postprandial pythons showed a significant increase in plasma total CO_2 after the consumption of a meal comprising 25% of their body weight (Fig. 1; $P < 0.001$). The increase in total CO_2 was highest at 1 day post feeding (dpf), reaching levels approximately 15 mM higher than those of fasted animals. By 4 dpf the postprandial alkaline tide had subsided with total CO_2 levels returning to fasting levels ($P > 0.05$). Kidney weight mass was significantly higher relative to body mass in 3 dpf pythons (3.62 ± 0.14 g) than fasted controls (2.7 ± 0.26 g) (data not shown; $P < 0.05$; ANCOVA).

The mRNA expression profiles of CA II, IV, XIII, V-type H^+ ATPase β-subunit, NHE3 and NBC were examined at 3 dpf as indicators of renal compensation after post-prandial alkaline tide (Fig. 2). Of the six genes, only CA IV showed a significant decrease in mRNA expression at 3 dpf ($P = 0.017$); however, both NHE3 and CA II showed significant up-regulation. No difference in total membrane-bound CA activity was found between fasted and 3 dpf pythons (Fig. 3a). In fasted animals the amount of CA activity released from the membranes was higher in PI-PLC treatments than vehicle controls ($P = 0.017$), while 3 dpf pythons showed no difference between PI-PLC and vehicle treatments ($P = 0.563$). This suggests the amount of GPI-linked CA in the kidney decreased post-feeding. Kidney cytoplasmic CA activity was not significantly different between fasted and fed snakes (Fig. 4a; $P = 0.07$), while V-type H^+ ATPase activity increased by approximately 2-fold (Fig. 4b; $P = 0.017$).

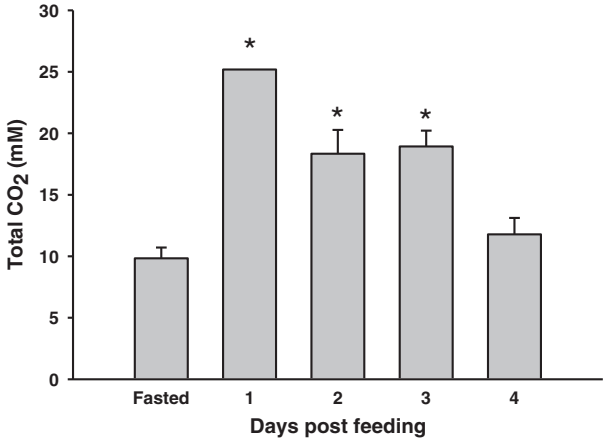

Fig. 1. Total plasma CO_2 in fasted and postprandial Burmese pythons. A significant difference from the fasted group is denoted by an asterisk (ANOVA, $P < 0.05$). All values are mean ± S.E.M. Fasted and 3 days post feeding, $N = 6$. Day 1, 2 and 4 post-feeding, $N = 2$.

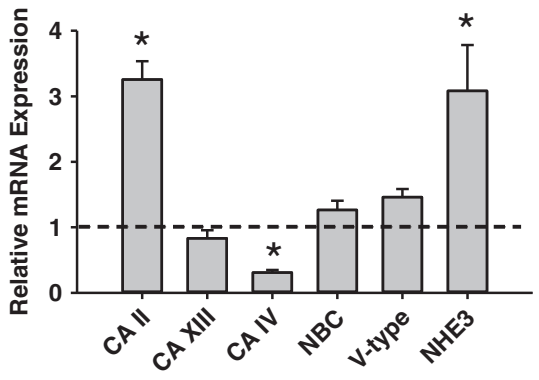

Fig. 2. The effect of feeding on gene expression in the kidney of Burmese pythons as detected by real-time RT-PCR. A significant difference between fasted and fed treatments is denoted by an asterisk (unpaired Student's *t*-test or Mann–Whitney rank sign test, $P < 0.05$). All values are mean ± S.E.M. $N = 5$–6.

3.2. Molecular analysis of carbonic anhydrase IV

Full length sequence information was obtained for a membrane-associated CA from the kidney of *P. molurus* and subsequent release of the *P. molurus* genome provided additional sequence information for four additional membrane isoforms. A series of phylogenetic analyses were performed to ensure proper sequence identity and to assess emerging trends pertaining to the expansion of membrane-bound CA isoforms in vertebrates (Fig. 5). The three analyses – maximum likelihood, maximum parsimony and neighbor joining – had generally similar topology. Of particular note was the presence of two CA IV isoforms in python, only one of which was expressed in the kidney (Fig. 1, arrow). Interestingly, two relatively well supported CA IV isoform groupings were apparent in the phylogenetic analyses, only one of which contained mammalian CA IV isoforms. Heretofore the second CA isoform is designated CA IV-like according to GenBank nomenclature.

Further in silico analysis of the python CA IV and CA IV-like amino acid sequences revealed a signal peptide ending at amino acid 21 and 22, respectively. Similarly, both isoforms contained a GPI-linkage site, which was located Ser-293 and Ser-296, respectively. To assess catalytic activity of the two isoforms the active site structure was compared to

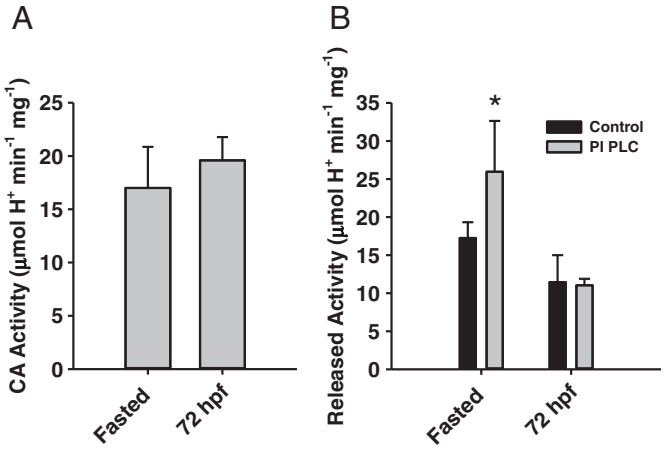

Fig. 3. A) Membrane-associated carbonic anhydrase activity in fasted and post-prandial Burmese python kidney homogenates. No significant differences were present between treatments (unpaired Student's *t*-test, $P < 0.05$; $N = 6$). B) The effects of PI-PLC on carbonic anhydrase membrane association in isolated kidney membranes from Burmese pythons. Significant release of carbonic anhydrase by PI-PLC relative to paired controls is denoted by an asterisk (paired Student's *t*-test, $P < 0.05$). All values are mean ± S.E.M ($N = 6$).

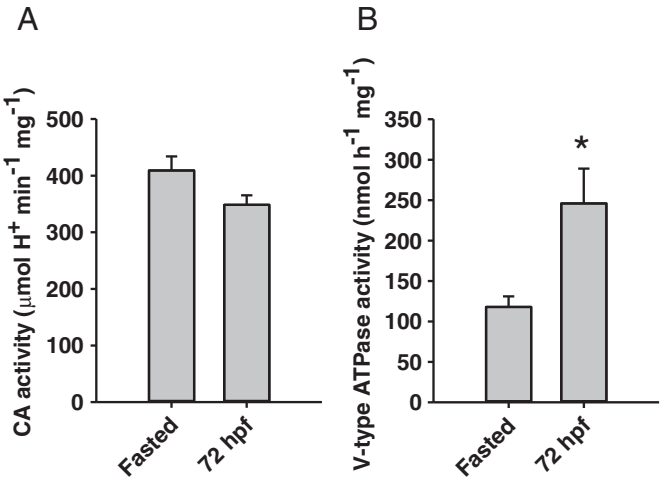

Fig. 4. A) Cytoplasmic carbonic anhydrase activity in fasted and post-prandial kidney homogenates. No significant differences were detected between treatments (unpaired Student's *t*-test; $P = 0.07$). B) V-type H^+ ATPase activity in fasted and post-prandial Burmese python kidney homogenates. A significant difference between fasted and fed treatments is denoted by an asterisk (unpaired Student's *t*-test, $P < 0.05$). All values are mean ± S.E.M ($N = 6$).

the high activity human CA II and IV isoforms (Table 2). Python CA IV deviated from the consensus high activity active site by only one more amino acid than human CA IV. This residue was not located at a crucial structural location. In contrast, python CA IV-like deviated by 5 additional amino acids including a crucial His/Lys-64 substitution.

4. Discussion

The primary mechanism of pH compensation following postprandial alkaline tide in Burmese pythons is a relative hypoventilatory response that reduces the amount of expired CO_2 relative to production (Overgaard et al., 1999; Hicks et al., 2000; Secor et al., 2000; Wang et al., 2001; Arvedsen et al., 2005). This process quickly re-establishes normal plasma pH values, but the plasma HCO_3^- concentrations would remain elevated. Nonetheless, a proxy for plasma HCO_3^- – total CO_2 – returned to fasting concentrations by 4 dpf (Fig. 1), which suggested that pythons in the current study were actively removing HCO_3^- from their blood stream during the post-feeding alkaline tide period. Undoubtedly there is an intestinal contribution, as intestinal alkalinisation rates are significantly elevated at 1 dpf; however, these rates returned to control levels at 2–4 dpf (Secor et al., 2012). While the current study was unable to directly measure urine HCO_3^- content due to the technical challenges associated with surgery and sample collection on post-fed snakes, we have provided evidence of renal re-modeling in the post-prandial period that would contribute to reduced HCO_3^- reabsorption.

The importance of reptilian kidneys for acid–base compensation is often downplayed. Alligator kidneys appear to be void of the cellular machinery necessary for HCO_3^- reabsorption (Ventura et al., 1989), and both turtles (*Chrysemms picta bellii*) (Silver and Jackson, 1986) and water snakes (*Nerodia sipedon*) (Dantzler, 1968) have shown no renal response to respiratory or metabolic acidosis, respectively. The current study shows that, unlike alligators, Burmese pythons have the cellular machinery required for renal acid–base homeostasis, including expression of CA II, CA IV, NHE3, NBC and V-type ATPase. Additionally, python kidneys also possess CA XIII, which has recently been suggested to assume the role of CA I in pythons (Esbaugh et al., 2015). The most notable finding in post-prandial pythons is an approximately 3-fold decrease in CA IV expression. This reduced expression was validated at the protein level using PI-PLC cleavage experiments, which are used to isolate the CA IV contribution in membrane fractions that may contain

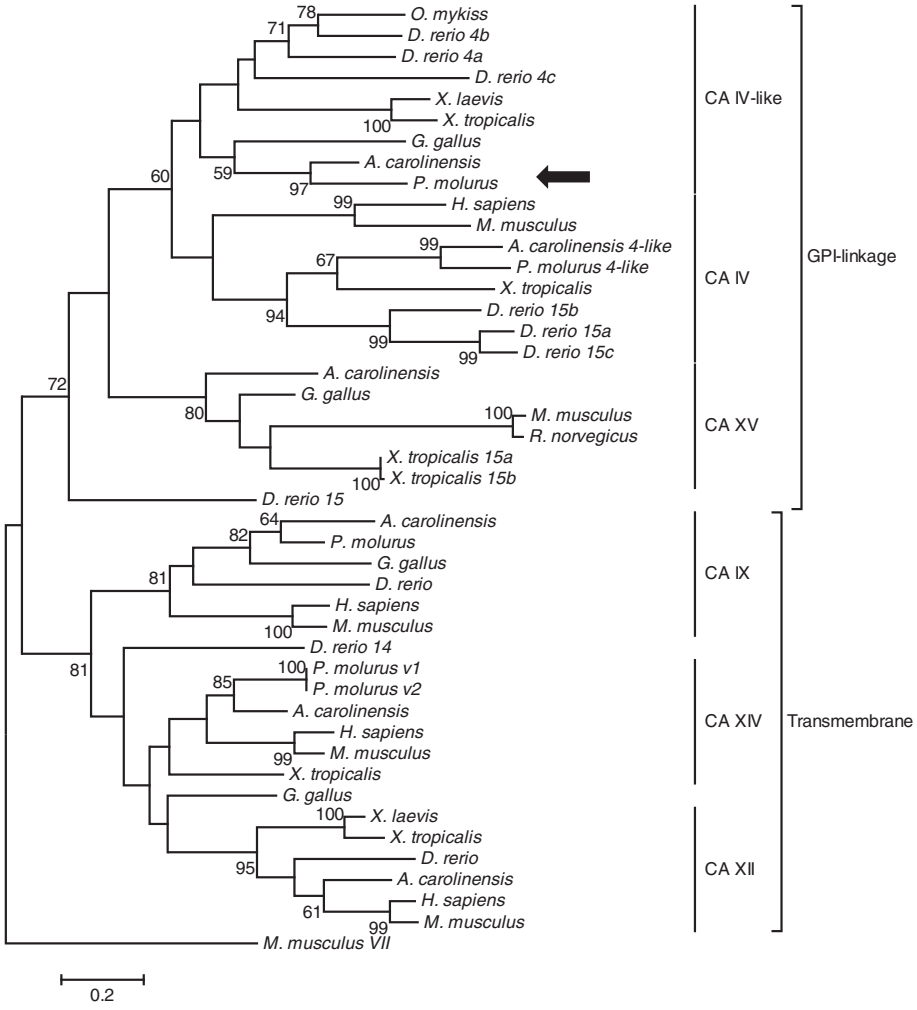

Fig. 5. A maximum likelihood phylogenetic reconstruction of the membrane-associated α-carbonic anhydrase isoforms. Bootstrap values for nodes are denoted with the exception of values below 50%, which indicates poor node support. The arrow designated the carbonic anhydrase IV isoform found in python kidneys. Additional numerical designation is provided for those sequences whose GenBank identification deviates from the phylogenetic reconstruction or to distinguish between multiple isoforms within a species. Similar tree topologies were obtained with neighbor joining and maximum parsimony reconstruction methods.

transmembrane CA isoforms or contaminating cytoplasmic isoforms. PI-PLC cleaves the GPI anchor that tethers CA IV to the apical membrane, and therefore treatment releases CA activity into the supernatant fraction during membrane isolation. Fasted python kidney membranes show increased release of activity when incubated with PI-PLC, relative to no enzyme controls, which demonstrates the presence of CA IV. However, no CA IV activity was detected in 72 h post-feeding snakes. These results clearly show that not only is CA IV activity present in the kidney, but that it is down-regulated during the post-prandial alkaline tide period.

Given the observed changes of CA IV expression and activity a series of phylogenetic and structural analyses were performed to ensure gene identity and function. This analysis also served to provide valuable information on the evolution of membrane α-CA isoforms as few such analyses have included reptile sequences. The recently published python genome (Castoe et al., 2011, 2013) provided information for five CA isoforms in addition to the CA IV obtained through homology cloning. Of these isoforms, three grouped within the transmembrane group of isoforms — most closely with CA XIV and CA IX. CA XIV is typically associated with heart, muscle and liver (Fujikawa-Adachi et al., 1999; Esbaugh and Tufts, 2004; Purkerson and Schwartz, 2005, 2007). With the exception of rodent species this isoform is not associated with the kidney (Mori et al., 1999; Purkerson and Schwartz, 2007). Similarly CA IX is not typically associated with the kidneys (Purkerson and Schwartz, 2007), although low expression has been documented in zebrafish (Esbaugh et al., 2009b). Interestingly, multiple CA IV isoforms were found in pythons as well as the amphibian *Xenopus tropicalis*. This had only previously been documented in teleosts (Lin et al., 2008), but it now appears that mammals may be unique with only a single isoform. Expression of only CA IV was detected in the python kidney, which is the CA IV isoform more distantly related to the mammalian isoform. From a structural perspective, only CA IV is consistent with a high activity isoform (Table 2). The CA IV-like isoforms contains a crucial substitution at His-64, which is the rate limiting proton shuttle residue and would greatly reduce turnover rate (Boone et al., 2014). This reduced activity is not common in vertebrates, as CA IV isoforms from hagfish to humans are predominantly high activity (Esbaugh and Tufts, 2006; Esbaugh et al., 2009a). The only two exceptions are rainbow trout and mice, and this has been linked to unique renal CA XIV expression in mice (Purkerson and Schwartz, 2007). Nonetheless, the CA IV expressed in the kidney of pythons is structurally representative of a high activity isoform.

Unlike many proteins in the kidney, CA IV expression and activity is simple to interpret owing to its singular role in HCO_3^- reabsorption. Therefore activity can be directly interpreted with respect to the effects on blood acid–base status. In fact, renal CA IV is often targeted pharmacologically to alleviate alkalosis, such as those common to altitude sickness (Swenson, 2000). Similar inhibition has also been demonstrated for snakes, whereby acetazolamide (a potent CA inhibitor) infusion

Table 2
Analysis of the putative active site pocket sequences for human and python carbonic anhydrase IV isoforms versus the high activity human carbonic anhydrase II. Numbers represent the location of each respective amino acid relative to alignment with human carbonic anhydrase II. Amino acid substitutions are designated by the respective amino acid letter, while no change is denoted by a dot.

Consensus II	Y	S	N	N	H	S	F	N	E	I	Q	H	H	E	H	V	F	L	V	G	W	Y	L	T	T	P	P	L	C	V	W	V	N	R
		7	29	61	62	64	65	66	67	69	91	92	94	96	106	107	117	119	121	131	141	143	145	192	194	198	199	200	201	202	204	206	207	209	211	244	246
						+							z	z				z	~		~	~				~	*						~	~			
Human IV		.	.	.	.	.	.	V	M	L	K	.	.	.	.	.	.	.	.	V	I	.	A	F	.	.	.	.	T	D	K	.	.	.	.
Python IV		.	.	.	.	.	T	V		Q	M	.	.	.	.	.	.	.	.	V	V	.	.	Y	.	.	.	.	G	N	E	.	.	L	.	.
Python IV-like		.	.	.	T	K	T	V	D	H	K	S	.	.	.	.	.	.	.	M	I	.	A	Y	.	.	.	.	G	D	A	.	.	I	.	.

z = zinc binding ligand.
+ = proton shuttling ligand.
~ = substrate associated pocket.
* = Thr-199 loop site.

resulted in alkaline urine in water snakes (Dantzler, 1968). These authors also demonstrated that metabolic alkalosis was accompanied by alkaline urine, although the mechanisms by which snakes increased urine alkalinisation were unknown. By reducing the amount of renal CA IV pythons likely increase the rate of urine alkalinisation versus fasted conditions, which likely contributes to the reduction of plasma HCO_3^- to control levels by 4 days post-feeding.

A confounding factor when interpreting post-prandial effects is the dual role that transport proteins play in renal salt and water absorption, both of which might be expected to increase post-feeding. This likely explains the up-regulation of NHE3 and CA II. From an acid–base perspective NHE3 expression would be expected to decrease in response to an alkalosis; however, NHE3 function is also related to renal Na^+ reabsorption. The absence of CA IV would further impact renal NHE3 function owing to micro-domain effects since CA IV would be unable to remove the transported proton through catalysis. This explanation also holds for cytoplasmic CA II because this enzyme provides the counter ions for not only NHE3 function, but also renal anion exchange related Cl^- transport. Conversely, V-type ATPase is not directly related to ion transport, although it does impact electrochemical gradients and thereby any electrogenic transport process. But V-type ATPase is crucially involved in α and β-intercalated cells of the collecting duct system. In α cells the V-type ATPase is apical oriented and involved in acid excretion into the lumen; however, the β cells contain basolateral ATPase that is critical for renal HCO_3^- secretion. It is tempting to suggest that the increased activity is related to increased proliferation of β cells, which has been documented during alkalosis in mammals. But this remains speculative and a clear area of future research regarding the renal remodeling of Burmese pythons post-feeding.

In summary, the current study demonstrated that the kidneys of Burmese pythons, unlike some reptiles (Ventura et al., 1989), contain all the components required for renal acid–base compensation, including a high activity CA IV isoform. Furthermore, CA IV expression and enzyme activity are significantly decreased after 3 dpf feeding compared to fasted controls, which corresponds to the period of plasma HCO_3^- recovery. While the well-documented hypoventilatory response immediately following feeding is central to maintaining plasma pH and protecting oxygen delivery, the current study presents a role for renal remodeling that may act to lower plasma HCO_3^- over the days following feeding and thereby stabilize blood CO_2 chemistry to control conditions. To our knowledge, the impact of feeding on glomerular filtration rate and urine production is unknown in pythons; however, a pronounced kidney hypertrophy has been previously demonstrated (Secor and Diamond, 1997b) and corroborated in the current study. This is indicative of increased organ activity, which authors had previously associated with increased nitrogenous waste production. Given the reduced capacity for HCO_3^- reabsorption in the absence of luminal CA IV, any increased kidney function would also serve to correct post-feeding pH disturbances.

Acknowledgments

Financial support for this work was provided by the Natural Science Foundation (NSF) grants to M. Grosell (IOS-11466695), S. Secor (IOS-0466139) and A.J. Esbaugh (EF-1315290). M. Grosell is a Maytag Professor of Ichthyology. Care of and experimentation on snakes were approved by the Institutional Animal Care and Use Committees of both the University of Alabama and the University of Miami.

References

Andrade, D.V., De Toledo, L.F., Abe, A.S., Wang, T., 2004. Ventilatory compensation of the alkaline tide during digestion in the snake Boa constrictor. J. Exp. Biol. 207, 1379–1385.
Arvedsen, S.K., Andersen, J.B., Zaar, M., Andrade, D., Abe, A.S., Wang, T., 2005. Arterial acid–base status during digestion and following vascular infusion of NaHCO(3) and HCl in the South American rattlesnake, *Crotalus durissus*. Comp. Biochem. Physiol. A Mol. Integr. Physiol. 142, 495–502.

Boone, C.D., Pinard, M., McKenna, R., Silverman, D., 2014. Catalytic mechanism of alpha-class carbonic anhydrases: CO_2 hydration and proton transfer. Subcell. Biochem. 75, 31–52.

Castoe, T.A., de Koning, J.A., Hall, K.T., Yokoyama, K.D., Gu, W., Smith, E.N., Feschotte, C., Uetz, P., Ray, D.A., Dobry, J., Bogden, R., Mackessy, S.P., Bronikowski, A.M., Warren, W.C., Secor, S.M., Pollock, D.D., 2011. Sequencing the genome of the Burmese python (*Python molurus bivittatus*) as a model for studying extreme adaptations in snakes. Genome Biol. 12, 406.

Castoe, T.A., de Koning, A.P., Hall, K.T., Card, D.C., Schield, D.R., Fujita, M.K., Ruggiero, R.P., Degner, J.F., Daza, J.M., Gu, W., Reyes-Velasco, J., Shaney, K.J., Castoe, J.M., Fox, S.E., Poole, A.W., Polanco, D., Dobry, J., Vandewege, M.W., Li, Q., Schott, R.K., Kapusta, A., Minx, P., Feschotte, C., Uetz, P., Ray, D.A., Hoffmann, F.G., Bogden, R., Smith, E.N., Chang, B.S., Vonk, F.J., Casewell, N.R., Henkel, C.V., Richardson, M.K., Mackessy, S.P., Bronikowski, A.M., Yandell, M., Warren, W.C., Secor, S.M., Pollock, D.D., 2013. The Burmese python genome reveals the molecular basis for extreme adaptation in snakes. Proc. Natl. Acad. Sci. U. S. A. 110, 20645–20650.

Cox, C.L., Secor, S.M., 2008. Matched regulation of gastrointestinal performance in the Burmese python, *Python molurus*. J. Exp. Biol. 211, 1131–1140.

Dantzler, W.H., 1968. Effect of metabolic alkalosis and acidosis on tubular urate secretion in water snakes. Am. J. Physiol. 215, 747–751.

Dantzler, W.H., Serrano, O.K., Abbott, D.E., Kim, Y.K., Brokl, O.H., 1999. Basolateral regulation of pHi in isolated snake renal proximal tubules in presence and absence of bicarbonate. Am. J. Physiol. 276, R1673–R1681.

Esbaugh, A.J., Tufts, B.L., 2004. Evidence for a membrane-bound carbonic anhydrase in the heart of an ancient vertebrate, the sea lamprey (*Petromyzon marinus*). J. Comp. Physiol. B. 174, 399–406.

Esbaugh, A.J., Tufts, B.L., 2006. The structure and function of carbonic anhydrase isozymes in the respiratory system of vertebrates. Respir. Physiol. Neurobiol. 154, 185–198.

Esbaugh, A.J., Gilmour, K.M., Perry, S.F., 2009a. Membrane-associated carbonic anhydrase in the respiratory system of the Pacific hagfish (*Eptatretus stouti*). Respir. Physiol. Neurobiol. 166, 107–116.

Esbaugh, A.J., Perry, S.F., Gilmour, K.M., 2009b. Hypoxia-inducible carbonic anhydrase IX expression is insufficient to alleviate intracellular metabolic acidosis in the muscle of zebrafish, *Danio rerio*. Am. J. Physiol. Regul. Integr. Comp. Physiol. 296, R150–R160.

Esbaugh, A.J., Secor, S.M., Grosell, M., 2015. Characterication of carbonic anhydrase XIII in the erythrocytes of the Burmese python, *Python molurus bivittatus*. Comp. Biochem. Physiol. B: Biochem. Mol. Biol. 187, 71–77.

Fujikawa-Adachi, K., Nishimori, I., Taguchi, T., Onishi, S., 1999. Human carbonic anhydrase XIV (*CA14*): cDNA cloning, mRNA expression, and mapping to chromosome 1. Genomics 61, 74–81.

Greene, H.W., 1997. Snakes: The Evolution of Mystery in Nature. California Press, Berkeley.

Henry, R.P., 1991. Techniques for measuring carbonic anhydrase activity in vitro. In: Dodgson, S.J., Tashian, R.E., Gros, G., Carter, N.D. (Eds.), The Carbonic Anhydrases: Cellular Physiology and Molecular Genetics. Plenum, New York, pp. 119–131.

Henry, R.P., Tufts, B.L., Boutilier, R.G., 1993. The distribution of carbonic anhydrase type I and II isozymes in lamprey and trout: possible co-evolution with erythrocyte chloride/bicarbonate exchange. J. Comp. Physiol. B. 163, 380–388.

Hicks, J.W., Wang, T., Bennett, A.F., 2000. Patterns of cardiovascular and ventilatory response to elevated metabolic states in the lizard Varanus exanthematicus. J. Exp. Biol. 203, 2437–2445.

Kim, Y.K., Dantzler, W.H., 1995a. Intracellular pH in snake renal proximal tubules. Am. J. Physiol. 269, R822–R829.

Kim, Y.K., Dantzler, W.H., 1995b. Relation of membrane potential to basolateral TEA transport in isolated snake proximal renal tubules. Am. J. Physiol. 268, R1539–R1545.

Kultz, D., Somero, G., 1995. Osmotic and thermal effects on in situ ATPase activity in permeabilized gill epithelial cells of the fish *Gillichthys mirabilis*. J. Exp. Biol. 198, 1883–1894.

Lin, H., Randall, D.J., 1993. H^+-ATPase activity in crude homogenates of fish gill tissue: inhibitor sensitivity and environmental and hormonal regulation. J. Exp. Biol. 180, 163–174.

Lin, T.Y., Liao, B.K., Horng, J.L., Yan, J.J., Hsiao, C.D., Hwang, P.P., 2008. Carbonic anhydrase 2-like a and 15a are involved in acid–base regulation and Na^+ uptake in zebrafish H^+-ATPase-rich cells. Am. J. Physiol. Cell Physiol. 294, C1250–C1260.

McCormick, S.D., 1993. Methods for non-lethal biopsy and measurement of Na^+, K^+ ATPase activity. Can. J. Fish. Aquat. Sci. 50, 656–658.

Mori, K., Ogawa, Y., Ebihara, K., Tamura, N., Tashiro, K., Kuwahara, T., Mukoyama, M., Sugawara, A., Ozaki, S., Tanaka, I., Nakao, K., 1999. Isolation and characterization of CA XIV, a novel membrane-bound carbonic anhydrase from mouse kidney. J. Biol. Chem. 274 (22), 15701–15705.

Ott, B.D., Secor, S.M., 2007. Adaptive regulation of digestive performance in the genus *Python*. J. Exp. Biol. 210, 340–356.

Overgaard, J., Busk, M., Hicks, J.W., Jensen, F.B., Wang, T., 1999. Respiratory consequences of feeding in the snake *Python molorus*. Comp. Biochem. Physiol. A Mol. Integr. Physiol. 124, 359–365.

Pfaffl, M.W., 2001. A new mathmatical model for relative quantification in real-time RT-PCR. Nucleic Acids Res. 29, 45.

Pope, C.H., 1961. The Giant Snakes. Knopf, New York.

Purkerson, J.M., Schwartz, G.J., 2005. Expression of membrane-associated carbonic anhydrase isoforms IV, IX, XII, and XIV in the rabbit: induction of CA IV and IX during maturation. Am. J. Physiol. Regul. Integr. Comp. Physiol. 288, R1256–R1263.

Purkerson, J.M., Schwartz, G.J., 2007. The role of carbonic anhydrases in renal physiology. Kidney Int. 71, 103–115.

Secor, S.M., 2003. Gastric function and its contribution to the postprandial metabolic response of the Burmese python *Python molurus*. J. Exp. Biol. 206, 1621–1630.

Secor, S.M., 2009. Specific dynamic action: a review of the postprandial metabolic response. J. Comp. Physiol. B. 179, 1–56.

Secor, S.M., Diamond, J., 1995. Adaptive responses to feeding in Burmese pythons: pay before pumping. J. Exp. Biol. 198, 1313–1325.

Secor, S.M., Diamond, J., 1997a. Determinants of the postfeeding metabolic response of Burmese pythons, *Python molurus*. Physiol. Zool. 70, 202–212.

Secor, S.M., Diamond, J., 1997b. Effects of meal size on postprandial responses in juvenile Burmese pythons (*Python molurus*). Am. J. Physiol. 272, R902–R912.

Secor, S.M., Diamond, J.M., 2000. Evolution of regulatory responses to feeding in snakes. Physiol. Biochem. Zool. 73, 123–141.

Secor, S.M., Nagy, K.A., 1994. Bioenergetics correlates of foraging mode for the snakes *Crotalus cerastes* and *Masticophis flagellum*. Ecology 1600–1614.

Secor, S.M., Hicks, J.W., Bennett, A.F., 2000. Ventilatory and cardiovascular responses of a python (*Python molurus*) to exercise and digestion. J. Exp. Biol. 203, 2447–2454.

Secor, S.M., Taylor, J.R., Grosell, M., 2012. Selected regulation of gastrointestinal acid–base secretion and tissue metabolism for the diamondback water snake and Burmese python. J. Exp. Biol. 215, 185–196.

Silver, R.B., Jackson, D.C., 1986. Ionic compensation with no renal response to chronic hypercapnia in *Chrysemys picta bellii*. Am. J. Physiol. 251, R1228–R1234.

Slip, D.J., Shine, R., 1988. Feeding habits of the diamond python, Morelia s. spilota: ambush predation by a boid snake. J. Herpetol. 323–330.

Swenson, E.R., 2000. Respiratory and renal roles of carbonic anhydrase in gas exchange and acid base regulation. In: Chegwidden, W.R., Carter, N.D., Edwards, Y.H. (Eds.), The Carboic Anhydrases: New Horizons. Birkhauser Verlag, Boston, pp. 281–342.

Toledo, L.F., Abe, A.S., Andrade, D.V., 2003. Temperature and meal size effects on the postprandial metabolism and energetics in a boid snake. Physiol. Biochem. Zool. 76, 240–246.

Ventura, S.C., Northrup, T.E., Schneider, G., Cohen, J.J., Garella, S., 1989. Transport and histochemical studies of bicarbonate handling by the alligator kidney. Am. J. Physiol. 256, F239–F245.

Wang, T., Busk, M., Overgaard, J., 2001. The respiratory consequences of feeding in amphibians and reptiles. Comp. Biochem. Physiol. A Mol. Integr. Physiol. 128, 535–549.